Synthesis and Characterization of Neutral and Cationic Magnesium Complexes Supported by NHC Ligands

Jean-Charles Bruyere, Christophe Gourlaouen, Lydia Karmazin, Corinne Bailly, Corinne Boudon, Laurent Ruhlmann, Pierre de Frémont, Samuel Dagorne

Synthesis and Characterization of Neutral and Cationic Magnesium Complexes Supported by NHC Ligands

Jean-Charles Bruyere,[†] Christophe Gourlaouen,[†] Lydia Karmazin,[‡] Corinne Bailly,[‡] Corinne Boudon,[†] Laurent Ruhlmann,[†] Pierre de Frémont,[†*] and Samuel Dagorne[†*]

[†] *Institut de Chimie de Strasbourg, CNRS - Université de Strasbourg, 1 rue Blaise Pascal, 67000 Strasbourg, France.*

[‡] *Service de Radiocristallographie - Fédération de Chimie Le Bel FR2010 – 1, rue Blaise Pascal - BP296/R8 - 67008 Strasbourg Cedex - France.*

RECEIVED DATE

For Table of Contents Only (Graphical Abstract)

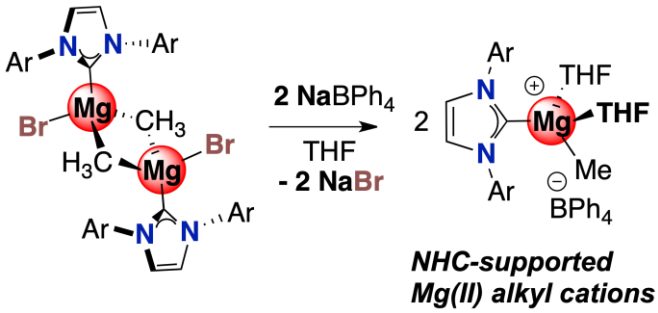

Abstract

A series of neutral N-heterocyclic carbene (NHC) magnesium alkyl complexes was synthesized by reaction of IMes (IMes = 1,3-bis(2,4,6-trimethylphenyl)imidazol-2-ylidene) and IPr (IPr = 1,3-bis(2,6-diisopropylphenyl)imidazol-2-ylidene) with Grignard reagents. In the presence of THF, mononuclear species [Mg(IMes)(R)(Br)(THF)] (**1**, R = Me; **2**, R = Et) and [Mg(IPr)(R)(Br)(THF)] (**3**, R = Me; **4**, R = Et) were isolated. Complex **4** was further methylated to afford the Mg–THF adduct [Mg(IPr)(Me)$_2$(THF)] (**5**) which crystallizes as dimer [{(Mg(IPr)(Me)}$_2$(μ-Me)$_2$] (**5'**), thus evidencing the labile THF coordination in these systems. In contrast, in the presence of Et$_2$O, dinuclear Mg(II) species [{(Mg(NHC)(Br)}$_2$(μ–Me)$_2$] (**6**, NHC = IMes; **7**, NHC = IPr), [{(Mg(IMes)(Ph)}$_2$(μ-Br)$_2$] (**8**), [{(Mg(IMes)(CH$_2$Ph)}$_2$(μ-Cl)$_2$] (**9**) and [{(Mg(IPr)(Ph)}$_2$(μ-Br)$_2$] (**10**) were isolated and characterized. The protonolysis reaction between protio-ligand [IMes-H]Cl and EtMgBr afforded the Mg(II) dihalido dimer [{(Mg(IMes)(Br)}$_2$(μ-Cl)$_2$] (**11**). The solid state molecular structures of species **5'**, **6**-**11** were established through X-ray crystallographic studies. THF adducts **1** and **3** may be readily ionized by a salt metathesis reaction with [BPh$_4$]Na in the presence of THF to yield NHC-supported Mg(II) alkyl cations [{Mg(NHC)(Me)(THF)$_2$}]$^+$ (**12**, NHC = IMes; **13**, NHC = IPr) as BPh$_4^-$ salts. Reflecting the labile THF coordination to Mg(II) in these cations, mononuclear cation **12** crystallizes as di-cation [{(Mg(IMes)(THF)}$_2$(μ-Me)$_2$]$^{2+}$ (**12'**). Only partial ionization of the halido methyl dimer **6** was observed by reaction with [B(C$_6$F$_5$)$_4$]Li in PhBr to afford tetranuclear NHC–Mg(II) di-cationic aggregate [{[Mg(IMes)(Me)][Mg(IMes)]}(μ-Me)$_2$]$_2$(μ-Br)$_2$]$^{2+}$ (**14**) as a B(C$_6$F$_5$)$_4$ salt. Computational studies were performed for selected neutral and cationic NHC–Mg(II) derivatives and all agree with the electronic structure and bonding at Mg(II) being largely dominated by electrostatic interactions.

Introduction

In 1900, Grignard described the synthesis of the ubiquitous and eponymous organomagnesium halide reagents.[1] Alkyl/aryllithium and alkyl/arylmagnesium species are since then widely used reagents in organic synthesis, essentially as alkylating and arylating stoichiometric reagents or co-catalysts.[3,4] Besides protolytic sensitivity, the preparation of well-defined organometallic complexes of Mg(II) is frequently complicated by ligand redistribution reactions in solution, also known as Schlenk equilibrium, due to their rather labile coordination of most monodentate ligands to Mg(II).[2,3] Thanks to their exceptional σ-donating properties, *N*-heterocyclic carbene ligands are of interest for the stabilization of various metal centers, leading to NHC-supported organometallics with improved stability that have found various applications across chemical science.[4] Though NHCs may stabilize oxophilic and electrophilic metal centers,[5] the M–NHC bond in such entities becomes increasingly labile with the electropositivity of the metal centers, which may significantly limit their stability and well-defined nature. Certainly related to the latter, the organometallic chemistry of NHC complexes of group *s* metals remains relatively unexplored compared to other main group metal/heteroatoms.[5,6] In particular, NHC magnesium complexes, first reported in 1993 by Arduengo,[7] have undergone a limited development, with an average of roughly a publication per year over the past 25 years.[5,8] With a monodentate NHC ligand, only a few examples of Mg-NHC adducts of the type (NHC)Mg(X)(X')$_2$, [(NHC)Mg–X']$_2$ (X, X' = alkyl, halide) as well as a couple of NHC-supported Mg(II) amido/hydrido species are thus far known.[8] Yet, from a general point of view, well-defined Mg(II) organometallics, which are thus based on an inexpensive and non-toxic metal center, are of potential interest for various stoichiometric and catalytic transformations of current importance.[8b,8g,9,10,11]

Well-defined Mg(II) organocations, which are typically supported by *N*-based multidentate ligand, are currently attracting attention as highly electrophilic and Lewis acidic Mg(II) species able to activate various unsaturated small molecules, including arenes, mediate unusual chemical transformations and be of potential interest in Lewis acid catalysis.[12] Following our earlier studies on NHC-stabilized Zn(II) organocations, which showed the ability of NHCs to stabilize two-coordinate Zn(II) cationic alkyls/aryls,[13] we became interested into probing the suitability of NHCs to access stable and robust NHC-stabilized Mg(II) organocations, a class of species unknown thus far. Along the way, a variety of NHC-stabilized Grignard reagents, used as

neutral precursors, were characterized allowing the establishment of structural trends. In the present contribution, we describe the synthesis and structural characterization of a variety of neutral NHC magnesium supported by halide- and alkyl/phenyl/benzyl-ligands. Some of these neutral precursors were then successfully ionized to NHC-stabilized Mg(II)–alkyl cations. The electronic structures of selected neutral and cationic complexes, as estimated from DFT calculations, complement their structural characterization.

Results and discussion

Synthesis and Structure of Neutral NHC-supported Mg(II) complexes 1-11. A diverse set of NHC-supported Mg–alkyl/aryl/benzyl halides were targeted to gain structural insights on such compounds prior to their subsequent ionization. The addition of an ethereal solution of ethylmagnesium bromide or methylmagnesium bromide to a THF solution of IMes (IMes = 1,3-bis(2,4,6-trimethylphenyl)imidazol-2-ylidene) or IPr (IPr = 1,3-bis(2,6-diisopropylphenyl)imidazol-2-ylidene) afforded complexes [Mg(IMes)(Et)(Br)(THF)] (**1**), [Mg(IMes)(Me)(Br)(THF)] (**2**), [Mg(IPr)(Et)(Br)(THF)] (**3**), or [Mg(IPr)(Me)(Br)(THF)] (**4**), in excellent yields (Scheme 1). ^{13}C NMR data confirmed the formation of Mg(II)−NHC bonds with $C_{carbene}$ chemical shifts comprised between 185 and 190 ppm.[8] The persistence of Mg(II)−alkyl bonds was confirmed by ^{1}H NMR spectroscopy (with high field signals ranging from -1.18 to -2.03 ppm). NMR data also agree with the coordination of a THF molecule per Mg(II) center. Complexes **1**-**4** are poorly soluble in benzene, toluene, or dichloromethane, but soluble and stable for weeks in THF at room temperature. Unfortunately, all attempts to crystallize THF adducts **1**-**4** remained unsuccessful.

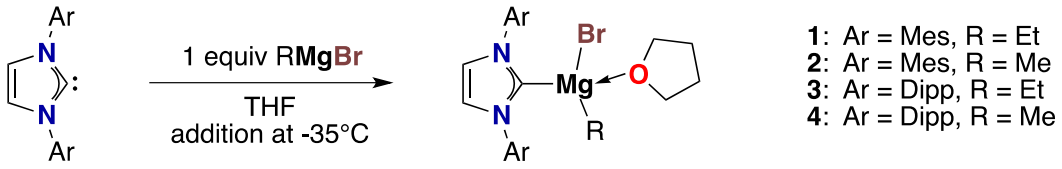

Scheme 1. Synthesis of the Mg complexes **1**-**4**

Species [Mg(IPr)(Me)(Br)(THF)] (**4**) was further methylated by reaction with methyllithium (THF, -35 °C) to form the corresponding dimethyl complex [Mg(IPr)$(Me)_2$(THF)]

(**5**, Scheme 2) in good yield (75%), as deduced from NMR data. In particular, the ^{1}H NMR spectrum for **5** displays a characteristic signal at -1.93 ppm associated with the Mg*Me*$_2$ moiety and resonances consistent with the coordination of a THF molecule. However, as determined by SC-XRD studies, species **5** crystallizes (from THF/pentane) as THF-free dimeric complex [{(Mg(IPr)(Me)}$_2$(μ-Me)$_2$] (**5'**, Figure 1), clearly indicating a labile THF coordination in parent complex **5** as also observed in a recent study on dihalido (NHC)MgX$_2$ species.[8h] Dimer **5'** features two NHC magnesium fragments linked by two μ-Me bridges. The two Mg(II) cations adopt a tetrahedral coordination geometry and the Mg1···Mg1' distance (2.7539(11) Å) is significantly shorter than the sum of their van der Waals radii (3.46 Å).[14] The Mg···Mg distance in **5'** is also intriguingly smaller than the Mg–Mg bond distances observed in Mg(I) dimers [(BDI)-Mg–Mg(BDI)] (BDI = *N*,*N* β-diketiminate), which range from 2.81(2) to 2.8656(2) Å.[15] The Mg–(μ-Me) bond distances (2.256(2) and 2.262(3) Å) are substantially longer than those of terminal Mg–Me bonds (2.141(2) Å). All geometrical parameters of **5'** are similar to those reported for the bridged dinuclear complex [{(Mg(IPr)(Et)}$_2$(μ-Et)$_2$] by Arduengo *et. al.*.[7]

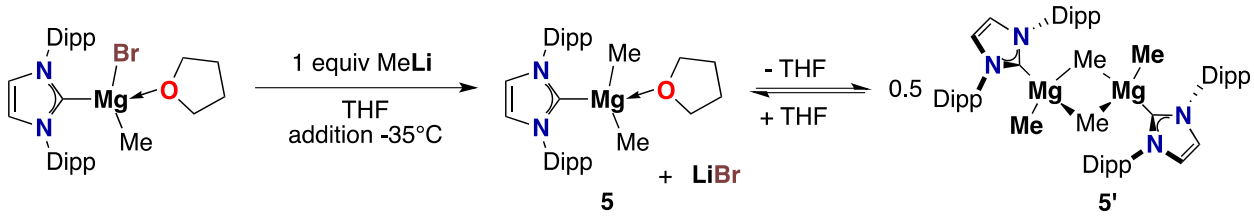

Scheme 2. Synthesis of THF adduct **5** and dimer **5'**

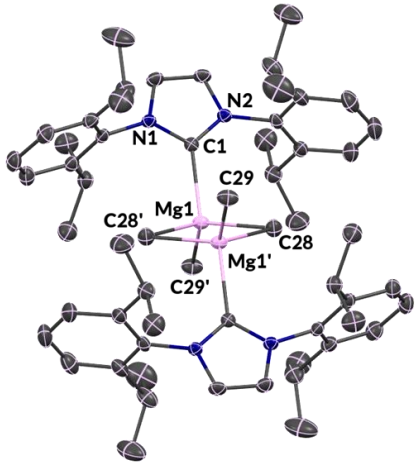

Figure 1. ORTEP representation of **5'** (30% probability). Hydrogen atoms have been omitted for clarity. Selected bond distances (Å) and angles (°): Mg1−C1 2.276(2), Mg1−C28 2.256(2), Mg1−C28' 2.263(2), Mg1−C29 2.141(2), C1−Mg1−C28 107.85(8), C1−Mg1−C28' 108.37(8), C1−Mg1−C29 105.74(7), C28−Mg1−C28' 104.89(7), C28−Mg1−C29 115.10(9), C28'−Mg1−C29 114.61(9).

In the absence of THF, the stoichiometric reaction of MeMgBr (Et_2O solution) with carbenes IMes and IPr (in toluene) led to the formation of dimeric complexes [{(Mg(IMes)(Br)}$_2$(μ-Me)$_2$] (**6**), [{(Mg(IPr)(Br)}$_2$(μ-Me)$_2$] (**7**) in good yields (Scheme 3), highlighting the key role of THF for the isolation of mononuclear NHC-Mg species **1**-**4**. For instance, the NMR data for **6** and **7** (C_6D_5Br, RT) confirm the presence of Mg–*Me* group with a ^{1}H NMR singlet at -1.96 ppm, and a ^{13}C NMR $C_{carbene}$ signal at 182.0 ppm in line with coordination to Mg(II). In the case of species **6**, ^{1}H DOSY NMR data agree with a dimeric structure in solution under the studied conditions (C_6D_5Br, RT). The hydrodynamic volume of **6** was estimated to be 1125 Å^3, which is close to the volume of dimeric **6** in the solid state (1150 Å^3) as estimated from SC-XRD data (*vide infra*). Both complexes **6** and **7** crystallize from toluene/pentane as dimers comprising two NHC magnesium fragments surprisingly linked by two bridging μ-Me groups instead of μ-Br bridges as would be expected (Figure 2 for complex **6**). Thus, a terminal Mg–*Br* completes the coordination sphere of each Mg(II) center. The Mg−C and Mg−halide bond lengths are in agreement with those found in the literature,[20] such as species [{(Mg(IPr)(I)}$_2$(μ-I)$_2$] and [{(Mg(IPr)(Cl)}$_2$(μ-Cl)$_2$] recently reported.[8f,8h] The structures of **6** and

7 highlight the preferential bridging of Me *vs.* halide groups and show that Et_2O does not dissociate dimers **6** and **7**, even though a magnesium dihalide complex supported by an abnormal NHC and an ether molecule is known.[8h] Similar to **5'**, the distance between the Mg(II) centers in **6** is equal to 2.750(4) Å. Alternatively, complex **6** was also prepared with a moderate yield (32 %) *via* reaction of 1 equiv of IMes with $MgCl_2$ followed by methylation with 1 equiv of MeLi.

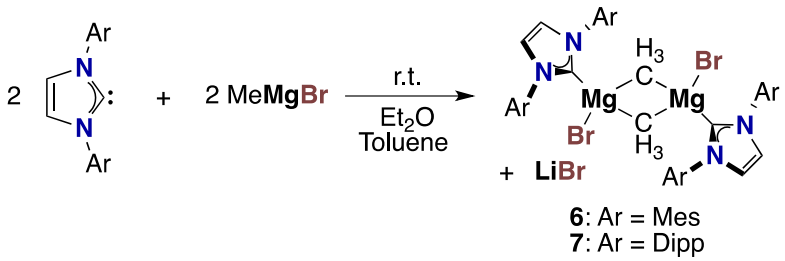

Scheme 3. Synthesis of species **6** and **7**

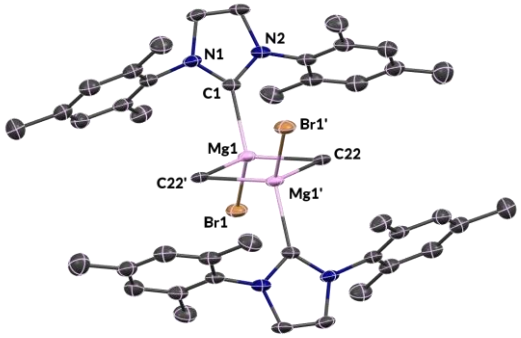

Figure 2. ORTEP representation of **6** (30% probability). Hydrogen atoms have been omitted for clarity. Selected bond distances (Å) and angles (°): Mg1−C1 2.214(6), Mg1−C22 2.313(6), Mg1−C22' 2.325(6), Mg1−Br1 2.4588(19), C1−Mg1−C22 108.8(2), C1−Mg1−C22' 108.7(2), C1−Mg1−Br1 112.63(17), C22−Mg1−Br1 109.58(15), C22'−Mg1−Br1 109.76(15), C22−Mg1−C22' 107.27(18).

To gain further knowledge on the structural trends of NHC-Mg(R)(X) species, the coordination of IMes and IPr was extended other classical Grignard reagents such as phenylmagnesium bromide, benzylmagnesium chloride. Thus, dimeric complexes $[\{(Mg(IMes)(Ph)\}_2(\mu\text{-}Br)_2]$ (**8**), $[\{(Mg(IMes)(Bn)\}_2(\mu\text{-}Cl)_2]$ (**9**) and $[\{(Mg(IPr)(Ph)\}_2(\mu\text{-}Br)_2]$

(**10**) were prepared in good yields (65-85%) upon combining a 1/1 mixture of the corresponding carbene and RMgX precursor in Et_2O/toluene. The molecular structures of species **8**-**10** were determined by SC-XRD establishing their dimeric nature in the solid state (Figure 3). Thus, unlike NHC-Mg(II) methyl halides dimers **6** and **7**, which contain two Mg-(*μ-Me*) groups, species **8**-**10** preferentially form *μ*-X halide bridges with the phenyl/benzyl groups as terminal ligands. Other bonding and geometrical parameters are similar to those observed for species **6** and **7**. The NMR data for species **8**-**10** are consistent with the proposed formulations.

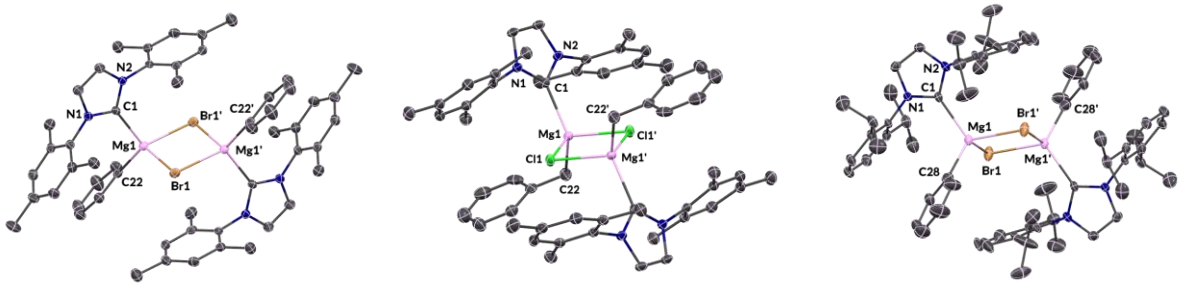

Figure 3: ORTEP representations of **8**, **9** and **10** (30% probability). Hydrogen atoms, and co-crystallized benzene for **8**, have been omitted for clarity. Selected bond distances (Å) and angles (°): for **8**: Mg1−C1 2.225(4), Mg1−C22 2.129(4), Mg1−Br1 2.5842(15), C1−Mg1−C22 115.07(15), C1−Mg1−Br1 112.38(11), C22−Mg1−Br1 112.55(12), Br1−Mg1−Br1' 92.57(4); for **9**: Mg1−C1 2.2065(15), Mg1−C22 2.1411(19), Mg1−Cl1 2.4224(7), Mg1−Cl1' 2.4341(7), C1−Mg1−C22 122.29(8), C1−Mg1−Cl1 107.77(4), C1−Mg1−Cl1' 109.20(4), C22−Mg1−Cl1 112.79(7), C22−Mg1−Cl1' 108.28(6), Cl1−Mg1−Cl1' 92.38(2); for **10**: Mg1−C1 2.216(2), Mg1−C28 2.280(2), Mg1−C28' 2.272(2), Mg1−Br1 2.4562(8), C1−Mg1−C28 112.48(8), C1−Mg1−C28' 112.36(8), C1−Mg1−Br1 105.91(6), C28−Mg1−Br1 110.15(6), C28'−Mg1−Br1 109.36(6), C28−Mg1−C28' 106.59(7).

Though NHC-Mg species are typically prepared from free NHC and Mg(II) precursors, they may directly be prepared through protonolysis of the imidazolium salts.[8f] Thus, protio ligand IMesHCl (1,3-bis(2,4,6-trimethylphenyl)imidazolium chloride) immediately reacts with 1 equiv EtMgBr (THF/Et_2O, 2 h, RT) through ethane elimination to afford dinuclear complex [{(Mg(IMes)(Br)}$_2$(*μ*-Cl)$_2$] (**11**, Scheme 4) in high yield (85%), as deduced from NMR and SC-XRD data. ^{1}H and ^{13}C NMR spectra confirm the formation of **11**, with the absence of the azolium proton signal, the presence of a ^{13}C NMR $C_{carbene}$ signal (δ = 187.0 ppm) and no THF moiety. In

the solid state, species **11** (Figure 4) is a dimer featuring two NHC magnesium fragments connected by two Mg-(μ-Cl)-Mg bridges, with bonding parameters in agreement with those found in the literature, particularly with complexes [{(Mg(IPr)(I)}$_2$(μ-I)$_2$] and [{(Mg(IPr)(Cl)}$_2$(μ-Cl)$_2$] recently reported.[8g,8h]

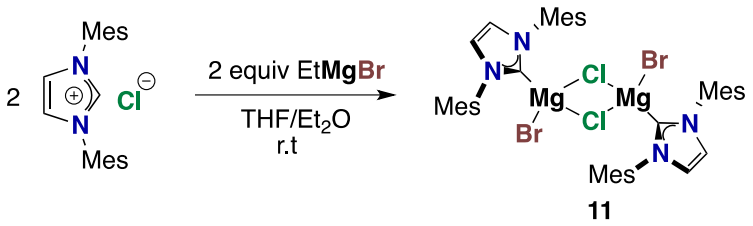

Scheme 4. Synthesis of species **11**

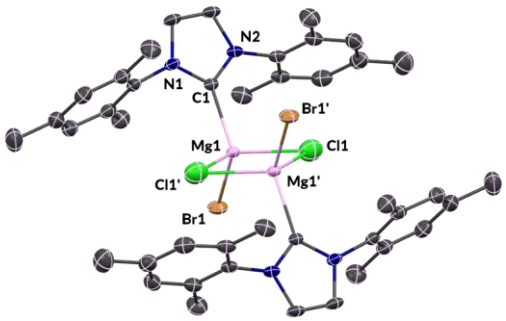

Figure 4. ORTEP representation of **11** (30% probability). Hydrogen atoms have been omitted for clarity. Selected bond distances (Å) and angles (°): Mg1−C1 2.211(5), Mg1−Cl1 2.372(3), Mg1−Br1 2.432(2), C1−Mg1−Cl1 108.52(9), C1−Mg1−Br1 113.16(17), Cl1−Mg1−Cl1' 107.72(13), Cl1−Mg1−Br1 109.39(6).

NHC-supported Mg–alkyl Cations. A primary aim of the present study was to access cationic NHC-supported Mg(II) alkyls from the set of neutral precursors characterized herein. Ionization of the dimethyl derivative [Mg(IPr)(Me)$_2$(THF)] with 1 equiv [Ph$_3$C][B(C$_6$F$_5$)$_4$] (C$_6$D$_5$Br, RT) immediately occurs through a Me$^-$ abstraction reaction (formation of Ph$_3$CMe evidenced by ^{1}H NMR), yet to consistently yield an intractable mixture of compounds in the presence or absence of additional THF. Rather, ionization of methyl halido derivatives

[(NHC)Mg(Me)(X)] through a salt metathesis route allowed access to well-defined Mg(II) cations. Thus, species **2** and **4** react with 1 equiv. Na[BPh_4] (PhF, RT) in the presence of 5 equiv. THF to afford the corresponding cations [{Mg(IMes)(Me)$(THF)_2$}]$^+$ (**12**) and [{Mg(IPr)(Me)$(THF)_2$}]$^+$ (**13**) as BPh_4^- salts (Scheme 5), along with a precipitate of NaBr, on the basis of ^{1}H, ^{13}C and ^{11}B NMR data. In particular, ^{1}H NMR data agree with the presence of a Mg–Me$^+$ moiety (δ = -1.62 and -1.70 ppm for **12** and **13**, respectively). The coordination of two THF molecules on Mg(II) for isolated salts **12** and **13** is indicated by significantly upfield shifted ^{1}H NMR resonances for Mg–*THF* (for instance, δ = 2.88 and 1.19 ppm for species **12**) relative to those of free THF (δ = 3.57 and 1.55 ppm). Also, the $C_{carbene}$ signals for **12** and **13** (δ = 179.1 and 181.6 ppm, respectively) are upfield shifted compared to those of parent precursors **2** and **4** (δ = 186.9 and 186.6 ppm), which is consistent with a more Lewis acidic Mg(II) center in cations **12** and **13**, as expected.[16] Salts **12** and **13**, isolated in good yield (over 80%) as colorless solids, are stable for weeks in the solid state and days in PhBr/PhF at room temperature under inert atmosphere. Both compounds are however unstable in CH_2Cl_2 and decompose within minutes at room temperature to unknown species.

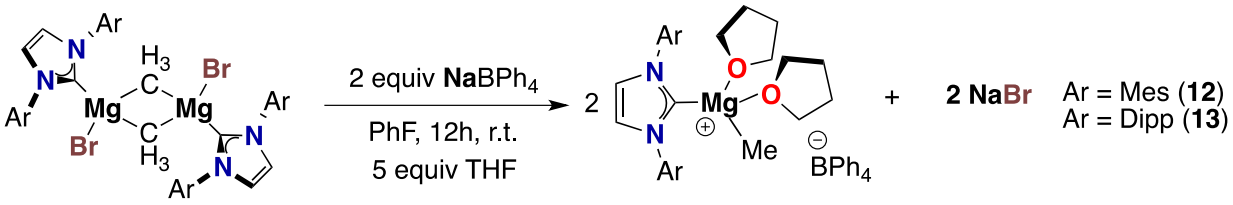

Scheme 5. Synthesis of NHC–Mg(II) alkyl cations **12-13**

The molecular structure of species **13** was confirmed by SC-XRD studies (Figure 5), indicating that its solution structure is retained in the solid state. It thus crystallizes as discrete [{Mg(IPr)(Me)$(THF)_2$}]$^+$ and BPh_4^- ions with no cation/anion interactions. The mononuclear cation features a central Mg(II) center lying in a distorted tetrahedral environment, resulting in C(1)-Mg(1)-C(28) and O(1)-Mg(1)-O(2) angles of 119.65(6) and 94.2(2)°, respectively. No significant differences were found in the Mg-NHC or Mg-Me bond lengths (Mg(1)-C(1) = 2.222(1), Mg(1)-C(28) = 2.133(2) Å) compared to neutral NHC-supported magnesium adducts. Interestingly, unlike **13**, crystallization of mononuclear cation **12** (from PhF/pentane) affords dinuclear di-cation [{(Mg(IMes)(THF)}$_2$(μ-Me)$_2$]$^{2+}$ (**12'**, Figure 6) as a BPh_4^- salt. Thus, despite Coulombic

repulsions, mono-cation **12** aggregates to form di-cation **12'** with concomitant loss of a THF molecule per Mg(II) center. The formation of **12'** clearly reflects both the labile THF coordination to Mg(II) in solution and the lower steric hindrance of IMes *vs.* IPr. Cation **12'** thus contains two Mg(II) centers lying in distorted tetrahedral environments with two μ-Me bridging ligands. Unlike neutral dimers discussed herein, the μ-Me groups in **12'** disymmetrically bridges the two Mg(II) centers leading to significantly different Mg–(μ-Me) bond lengths: for instance, Mg1–C22 = 2.205(4) and Mg1–C22' = 2.338(4) Å. As a comparison, the Mg–(μ-Me) bond lengths are nearly identical in neutral dimer **6** [{(Mg(IMes)(Cl)}$_2$(μ-Me)$_2$] (Figure 2, Mg1−C22 = 2.313(6), Mg1−C22' = 2.325(6)). The observed bonding parameters in Mg–(μ-Me)–Mg bridges of **12'** with rather long Mg1−C22' and Mg1'–C22 distances may be sterically and electronically driven: *i.e.* to limit steric hindrance and Coulombic repulsions.

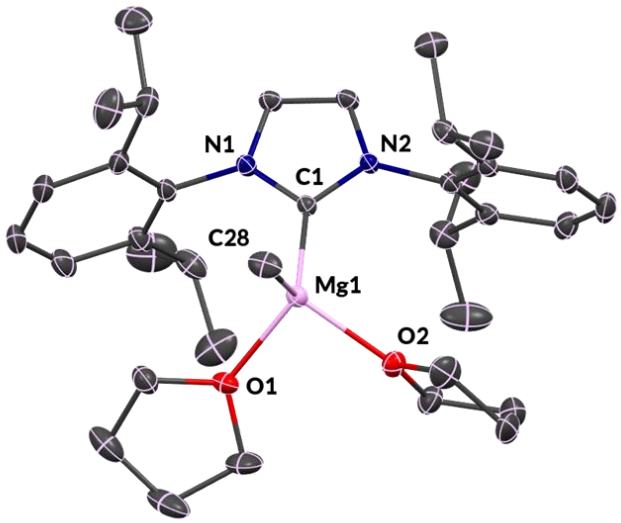

Figure 5. ORTEP representation of **13** (30% probability). The anions and hydrogen atoms have been omitted for clarity. Selected bond distances (Å) and angles (°): Mg1−C1 2.2224(13), Mg1−C28 2.1334(15), Mg1−O1 2.0309(12), Mg1−O2 2.045(7), C1−Mg1−C28 119.65(6), C1−Mg1−O1 111.43(5), C1−Mg1−O2 109.82(18), O1−Mg1−O2 94.19(13).

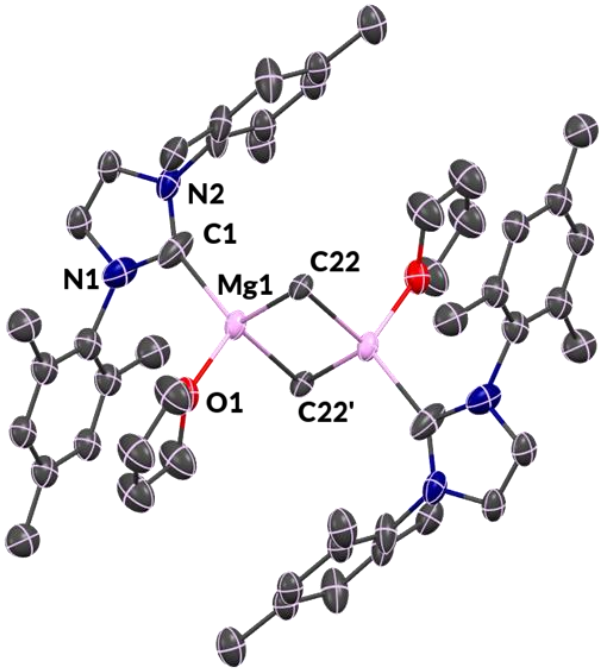

Figure 6: ORTEP representation of **12'** (30% probability). The anions and hydrogen atoms have been omitted for clarity. Selected bond distances (Å) and angles (°): Mg1−C1 2.275(6), Mg1−C22 2.205(4), Mg1−C22' 2.338(4), Mg1−O1 2.006(7), C1−Mg1−C22 117.3(2), C1−Mg1−C22' 109.4(2), C1−Mg1−O1 117.6(3), C22−Mg1−O1 100.5(2), C22'−Mg1−O1 104.3(2), C22−Mg1−C22' 106.42(14).

The ionization of dimers [{(Mg(IMes)(Br)}$_2$(μ-Me)$_2$] (**6**) and [{(Mg(IPr)(Br)}$_2$(μ-Me)$_2$] (**7**) was also investigated in the absence of any external Lewis base. No reaction was observed between derivative **6** or **7** and 2 equiv Na[BPh$_4$] (PhBr or PhF, room temperature, 24 h) due to the poor solubility of all reagents, leading us to the use of the more soluble salt reagent Li[B(C$_6$F$_5$)$_4$] as an ionizing agent. An initial monitoring NMR scale reaction of a 1/2 **6**/Li[B(C$_6$F$_5$)$_4$] mixture (C$_6$D$_5$Br, 12 h, room temperature) led to the quantitative formation of polynuclear Mg(II) di-cation [{[Mg(IMes)(Me)][Mg(IMes)]}(μ-Me)$_2$]$_2$(μ-Br)$_2$]$^{2+}$ as a B(C$_6$F$_5$)$_4^-$ salt (**14**, Scheme 6), along with 1 equiv of unreacted Li[B(C$_6$F$_5$)$_4$] and formation of a precipitate attributed to LiBr. Heating the reaction mixture (50 °C, 2 h) to promote further ionization only led to decomposition products. The generation of cation **14** likely proceeds by a Br$^-$ abstraction from dimer [{(Mg(IMes)(Br)}$_2$(μ-Me)$_2$] to afford transient dinuclear mono-cation [{(Mg(IMes)}$_2$(μ-Me)$_2$(Br)]$^+$ that then dimerizes to di-cation **14** through formation of two Mg–(*μ-Br*)–Mg bridges.

Compound **14** was isolated as colorless crystals in low yield (22 %) from reaction of a 1/1 **6**/Li[B(C_6F_5)$_4$] mixture.

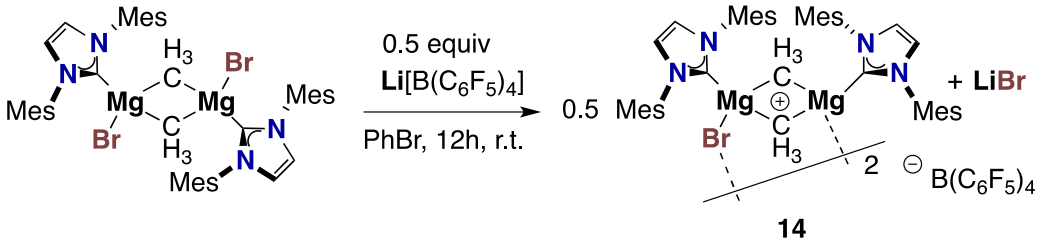

Scheme 6. Synthesis of the tetranuclear NHC–Mg(II) cationic complex **14**

The molecular structure of **14**, as established through SC-XRD analysis, consists of discrete [{[Mg(IMes)(Me)][Mg(IMes)]}(μ-Me)$_2$]$_2$(μ-Br)$_2$]$^{2+}$ (Figure 7) and B(C_6F_5)$_4^-$ ions with no cation/anion interactions. The di-cation is comprised of two IMes–Mg(II) fragments connected by two μ-Me moieties and further assembled by two additional μ-Br groups. This results into a C_{2v}-symmetric central tetranuclear [(μ-Br)Mg(μ-Me)$_2$Mg]$_2$ core with each metal center being decorated by a IMes carbene ligand. The Mg(II) centers are four-coordinate and lie in a slightly distorted tetrahedral environment with, for instance, C(1)-Mg(1)-Br(1) and Mg(1)-C(44)-Mg(1) angles of 108.0(2) and 104.7(3)°, respectively. The Mg–NHC bond lengths (2.209(6) and 2.187(6) Å) are similar to those of the neutral parent compound **2**. The ^{1}H and ^{13}C NMR data for **14** (C_6D_5Br, room temperature) agree with a C_{2v}-symmetric cationic species, with only one set of NMR resonances for the Mg–*Me* and IMes moieties. The ^{13}C NMR $C_{carbene}$ signal (δ = 175.3 ppm) is consistent with IMes coordination to Mg(II).

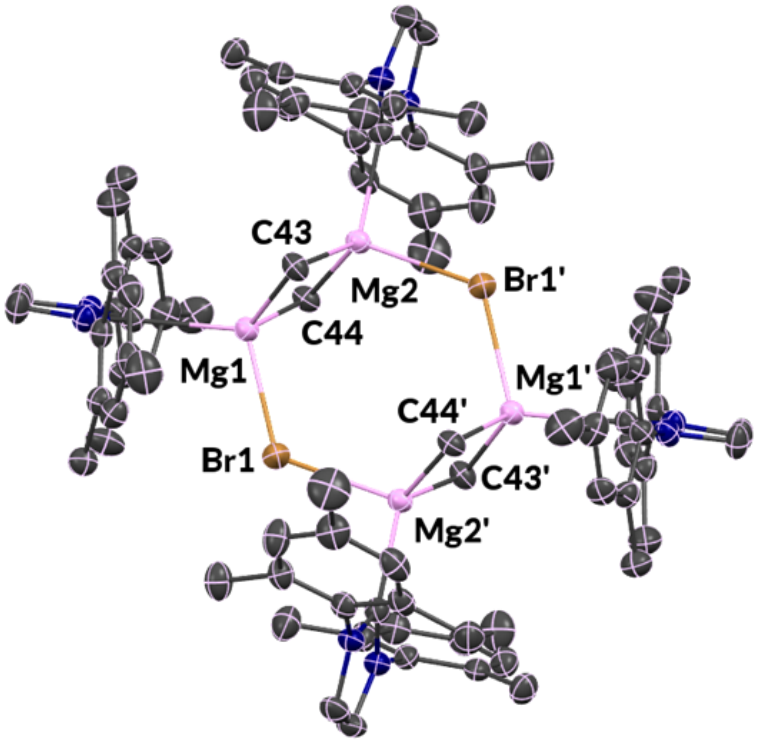

Figure 7. ORTEP representation of **14** (30% probability); the anions $B(C_6F_5)_4^-$ and hydrogen atoms have been omitted for clarity. Selected bond distances (Å) and angles (°): Mg1−C1 2.210(6), Mg1−C43 2.234(6), Mg1−C44 2.263(7), Mg1−Br1 2.5204(19), Mg2−C22 2.186(6), Mg2−C43 2.240(7), Mg2−C44 2.231(6), C1−Mg1−Br1 107.97(16), C1−Mg1−C43 113.4(2), C1−Mg1−C44 117.2(3), C43−Mg1−Br1 107.3(2), C44−Mg1−Br1 105.72(17), C22−Mg2−C43 118.2(2), C22−Mg2−C44 114.5(2), C43−Mg1−C44 104.6(2), C43−Mg2−C44 105.5(2).

In preliminary reactivity studies, cationic Mg–NHC alkyls **12** and **13** were observed to react fast and quantitatively with 1 equiv. of $PhSiH_3$ (THF-d^8 or C_6D_5Br, 5 min, room temperature) through presumably an alkyl-hydride exchange reaction (as deduced from the quantitative formation of $PhEtSiH_2$), a reactivity well-established for neutral Mg–alkyl species.[17] Yet, the putatively formed Mg–H species are instable under the studied conditions to decompose to insoluble and unidentified material.[18]

DFT-estimated electronic structure of NHC-supported Mg(II) species. The electronic structure and bonding features of selected neutral and cationic Mg-NHC species prepared herein were DFT-computed. First, as estimated at the PBEPBE/6-31+G** theory level,[19,20] the bonding

and geometrical parameters at the Mg(II) centers for model compounds[21] [{(Mg(IPr)(Me)}$_2$(μ-Me)$_2$] (**V'**), [{(Mg(IMes)(Br)}$_2$(μ-Me)$_2$] (**VI**), [{(Mg(IPr)(Br)}$_2$(μ-Me)$_2$] (**VII**), [{(Mg(IMes)(THF)}$_2$(μ-Me)$_2$]$^{2+}$ (**XII'**), [{Mg(IPr)(Me)(THF)$_2$}]$^+$ (**XIII**) agree well with SC-XRD-characterized species **5'**, **6**, **7** and **12'** and **13** (Table S1, Supporting Information). For all species, NBO analysis of the bonding at Mg(II) are consistent with essentially ionic Mg–alkyl and Mg–NHC bonds with Wiberg indexes (WI) ranging from 0.22 for the Mg–(μ-Me) bonds in **V'** to 0.35 for the Mg–Me bond in di-cation **XII'** (Table S2, Supporting Information). The bonding of terminal ligands to Mg(II) is a bit more covalent as reflected by WI values of 0.38, 0.53 and 0.56 for, respectively, the Mg–Me bond in **V** and the Mg–Br bonds in **VI** and **VII**. The positive charge at Mg(II) ranges from 1.12 to 1.25 for neutral models and is of 1.35 and 1.40 for cations **XII'** and **XIII**, respectively, in line with a more electro-deficient Mg(II) center upon cationization. The overall electrostatic bonding of the model Mg(II) complexes was further supported by the electron localization function (ELF) topological analysis (Table S3, Supporting Information). As deduced from ELF isosurfaces computed for model **V'** (Figure 8), no valence basins was identified between the Mg(II) center and the supporting ligands (bridging or terminal Me$^-$ and IPr). A minor covalent character is present in the Mg–Br bonds as shown by the presence of a Mg-Br valence basin. However, these basins can be considered as ligand lone pair with a neglectable electronic contribution of the Mg(II) cation to these basins (Table S3).

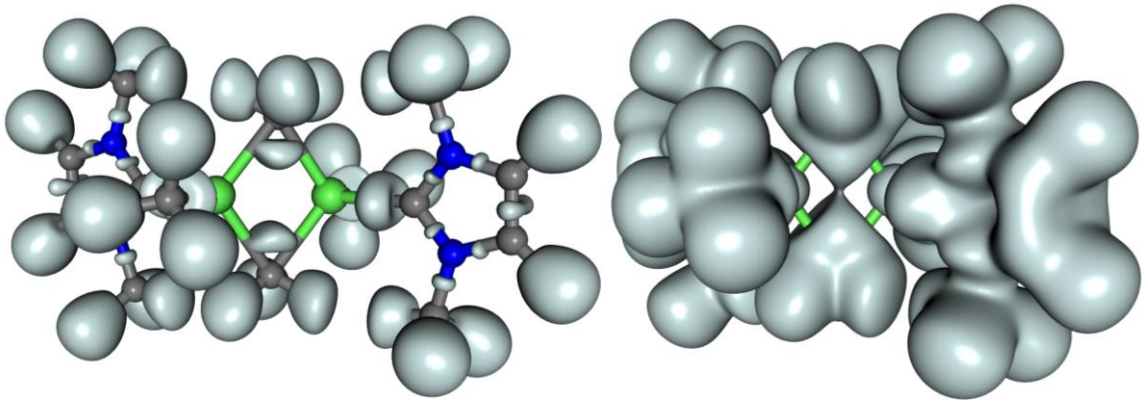

Figure 8. Electron Localization Funtion (ELF) isosurface (left, η = 8.87; right, η = 0.27) for a simplified model of **V** (the *N*-Dipp are replaced by *N*-Me groups for shorter calculation time).

Non Covalent Interactions (NCI) analyses were also computed and further support the predominance of attractive electrostatic forces for Mg(II)-ligand interactions, as illustrated in the

case of model **V'** (Figure 9). Interestingly, the NCI and ELF data for **V'** also provide a rationale to the rather short Mg···Mg distances observed for all structurally characterized NHC–Mg dimers. Thus, as shown in Figure 9, the NCI for **V'** feature repulsive and attractive forces between the Mg(II) centers, while only Coulombic repulsion would be expected between cations. Yet, from the ELF plot (Figure 8), the lone pair basins of the bridging Me groups connect at low isosurface value suggesting the presence of electron density between the Mg(II) centers. Such density arising from the two μ-Me groups results in Coulombic attraction with both Mg(II) centers, hence a shorter Mg–Mg distance than expected.

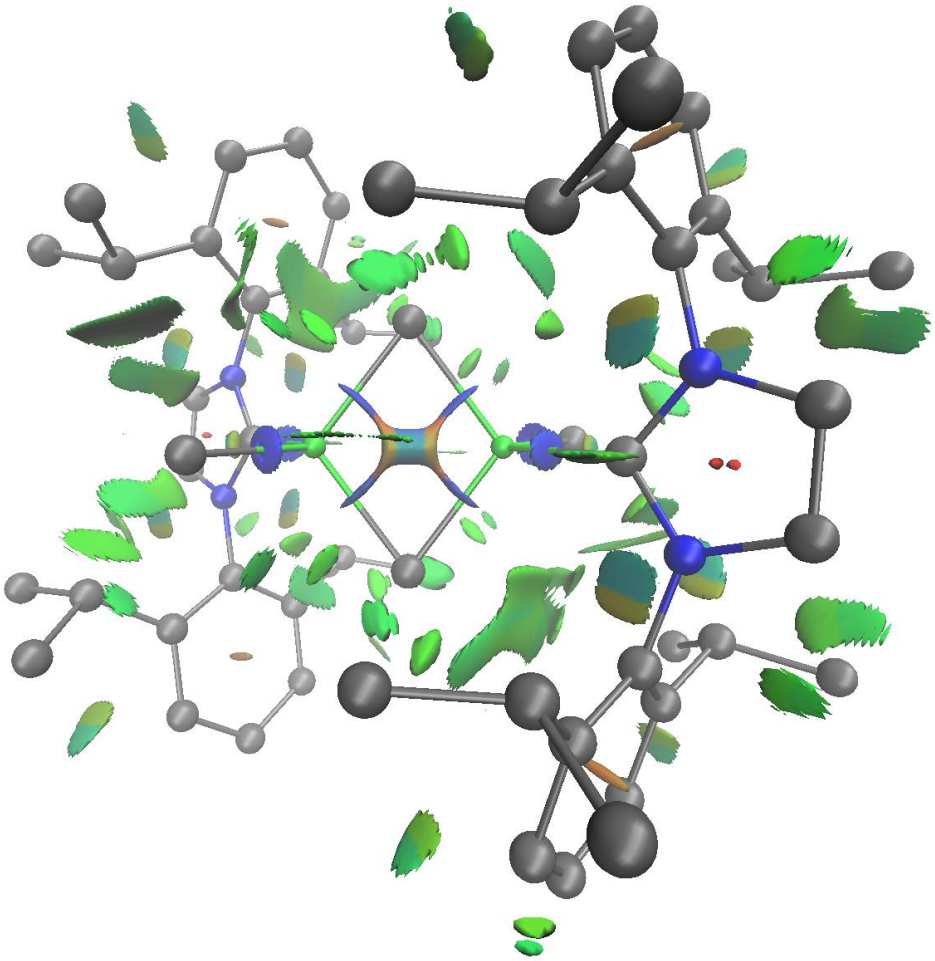

Figure 9. Non Covalent Interactions (NCI) analysis for model species **V'**. Hydrogen atoms are omitted for clarity. The green basins represent area where attractive dispersive forces are present. The blue basins show the presence of attractive electrostatic forces. In red are displayed areas of steric clashes.

Conclusion

A series of neutral complexes NHC-supported Grignard reagents and dialkyl Mg(II) species were synthesized and thoroughly structurally characterized, further establishing their strong tendency towards aggregation with the formation of $[(NHC)Mg(R)(X)]_2$ dimeric adducts. Though mononuclear Mg–THF adducts [(NHC)Mg(R)(X)(THF)] may be isolated, all data suggest that THF coordination to Mg(II) is labile as reflected by the characterization of dimeric adduct **5'** from mononuclear THF adduct **5**. These Grignard NHC adducts were successfully ionize to cationic NHC magnesium alkyls through halide abstraction. Akin to their neutral parent precursors, the structure of the resulting cations is strongly dependent upon reaction medium. The presence of THF allowed access to mononuclear NHC-supported Mg–alkyl cations **12** and **13**. The labile nature of the Mg–THF interaction in such cations was also clearly evidenced with the formation of dimeric di-cation **12'** arising from aggregation of *bis*-THF mono-cation **12**. Accordingly, carrying the ionization [(NHC)Mg(R)(X)]-type species in the absence of THF may lead to larger cationic aggregates, as illustrated by the formation of tetranuclear NHC–Mg(II) di-cation **14**. As computed for selected neutral and cationic derivatives, the bonding at Mg(II) is essentially dominated by electrostatic interactions, which also rationalizes the rather short Mg···Mg distances systematically observed in all structurally characterized Mg(II) dimers.

Experimental Section

General considerations

All experiments were carried out under N_2 using standard Schlenk techniques or in a MBraun Labmaster l30 glovebox. Toluene and pentane were collected after going through drying columns (MB SPS-800), then distilled under N_2 (over Na/benzophenone, or CaH_2), and stored at last over molecular sieves (4 Å) for 24 h in a glovebox prior to use. All deuterated solvents were purchased from Sigma-Aldrich, excepted for C_6D_5Br, purchased from ABCR GmbH & Co. They were stored over molecular sieves (4 Å) for 24 h prior to use. Anhydrous $MgBr_2$ was purchased from Strem Chemicals and used as received. Methyllithium 1.6 M in Et_2O, Grignard Reagent

Solutions (EtMgBr, BnMgCl at 1.0 M and MeMgBr, PhMgBr at 3.0 M, in Et_2O) were all purchased from Sigma-Aldrich and used as received. IMesHCl, IPrHCl, IMes, and IPr were prepared according to literature procedures.[22] All NMR measurements were performed with Teflon-valve J. Young NMR tubes at ambient conditions. Proton (^{1}H NMR) and carbon (^{13}C{^{1}H} NMR) nuclear magnetic resonance spectra were recorded on the following instrument: Bruker AVANCE I – 500 MHz spectrometer. The chemical shifts are given in part per million (ppm). Chemical shifts are given in ppm, ^{1}H and ^{13}C shifts are reported towards $SiMe_4$, and were determined relative to the residual signals of deuterated solvents as internal references, while ^{19}F and ^{11}B NMR shifts are reported respectively towards BF_3 and H_3BO_3 as external references. Data are presented as follows: chemical shift, multiplicity (s = singlet, d = doublet, t = triplet, q = quartet, sept = septuplet, m = multiplet, br = broad), coupling constants (J/Hz) and integration. For the X-ray diffraction studies, the intensity data were collected at 173(2) K on a Bruker KAPPA APEX II DUO diffractometer or on a Bruker KappaCCD diffractometer (compound **8**). Crystallographic and experimental details for all the structures are summarized in the Supporting Information (page S17). The structures were solved by direct methods (SIR-97 or SHELXS-2013 or SHELXS-2014) and refined by full-matrix least-squares procedures (based on F^2, SHELXL-2013 or SHELXL-2014) with anisotropic thermal parameters for all the non-hydrogen atoms.[23,24] The hydrogen atoms were introduced into geometrically calculated positions (SHELXL-2013 or SHELXL-2014 procedures) and refined riding on the corresponding parent atoms. Despite numerous attempts and akin to previous reports, satisfactory elemental analyses could not be collected for the NHC magnesium complexes due to their very sensitive nature.[8h,8i]

Preparation of [Mg(IMes)(Et)(Br)(THF)] (1). In a glovebox, 1.05 equiv. of ethylmagnesium bromide in Et_2O solution (1.00 ml, 0.99 mmol) was added dropwise to a cold solution of THF (-35 °C) containing 1 equiv. of free IMes (0.287 g, 0.94 mmol). The mixture was stirred for 4 hours at room temperature. Then, THF was removed under reduced pressure, and the resulting white powder was washed with 10 ml of pentane to afford complex **1** (0.451 g, 96 %).^{1}H NMR (500 MHz, d_8-THF): -1.18 (q, ^3J = 7.7 Hz, 2H, MgEt), 0.82 (t, ^3J = 7.7 Hz, 3H, MgEt), 1.77 (m, 4H, THF), 2.15 (s, 12H, Ar(*o*-Me)), 2.33 (s, 6H, Ar(*p*-Me)), 3.62 (m, 4H, THF), 7.02 (s, 4H, Ar(*m*-H)), 7.27 (s, 2H, Im(H)); ^{13}C NMR (125 MHz, d_8-THF): -1.1 (MgEt), 13.4 (MgEt), 18.0 (Ar(*o*-Me)), 20.9 (Ar(*p*-Me)), 26.2 (THF), 68.0 (THF), 123.4 (Im(CH)), 129.6 (Ar(CH)), 136.3 (Ar), 137.0 (Ar), 139.3 (Ar(C_{ipso})), 187.2 (carbene).

Preparation of [Mg(IMes)(Me)(Br)(THF)] (2). Following a protocol used for **2**, 1.05 equiv. of methylmagnesium bromide in Et_2O solution (0.7 ml, 2.10 mmol) and 1 equiv. of free IMes (0.506 g, 1.99 mmol) produced complex **3** as an off-white powder (0.953 g, 96 %). ^{1}H NMR (500 MHz, d_8-THF): -2.03 (s, 3H, MgMe), 1.77 (m, 4H, THF), 2.15 (s, 12H, Ar(*o*-Me)), 2.33 (s, 6H, Ar(*p*-Me)), 3.62 (m, 4H, THF), 7.01 (s, 4H, Ar(*m*-H)), 7.27 (s, 2H, Im(H)); ^{13}C NMR (125 MHz, d_8-THF): -15.4 (MgMe), 18.0 (Ar(*o*-Me)), 20.9 (Ar(*p*-Me)), 26.2 (THF), 68.0 (THF), 123.4 (Im(CH)), 129.5 (Ar(CH)), 136.3 (Ar), 136.7 (Ar), 139.3 (Ar(C_{ipso})), 186.9 (carbene).

Preparation of [Mg(IPr)(Et)(Br)(THF)] (3). Following a protocol used for **2**, 1.06 equiv. of ethylmagnesium bromide in Et_2O solution (0.9 ml, 0.92 mmol) and 1 equiv. of free IPr (0.340 g, 0.87 mmol) produced complex **3** as an off-white powder (0.411 g, 95 %). ^{1}H NMR (500 MHz, d_8-THF): -1.18 (m, 2H, MgEt), 0.85 (m, 3H, MgEt), 1.15 (d, ^3J = 6.7 Hz, 12H, CH_3-*i*Pr), 1.29 (d, ^3J = 6.7 Hz, 12H, CH_3-*i*Pr), 1.77 (m, 4H, THF), 2.84 (sp, ^3J = 6.7 Hz, 4H, CH-*i*Pr), 3.62 (m, 4H, THF), 7.31 (d, ^3J = 7.7 Hz, 4H, Ar(*m*-H)), 7.34 (s, 2H, Im(H)), 7.42 (t, ^3J = 7.7 Hz, 2H, Ar(*p*-H)); ^{13}C NMR (125 MHz, d_8-THF): -1.2 (MgEt), 13.5 (MgEt), 23.9 (CH_3-*i*Pr), 25.6 (CH_3-*i*Pr), 26.1 (THF), 29.1 (CH-*i*Pr), 68.0 (THF), 124.2 (Im(CH)), 124.4 (Ar(CH)) 130.0 (Ar(CH)), 137.6 (Ar), 146.7 (Ar(C_{ipso})).

Preparation of [Mg(IPr)(Me)(Br)(THF)] (4). Following a protocol used for **2**, 1.05 equiv. of methylmagnesium bromide in Et_2O solution (0.5 ml, 1.57 mmol) and 1 equiv. of free IPr (0.582 g, 1.50 mmol) produced complex **4** as a white powder (0.717 g, 97 %). ^{1}H NMR (500 MHz, d_8-THF): -2.03 (s, 3H, MgMe), 1.15 (d, ^3J = 6.6 Hz, 12H, CH_3-*i*Pr), 1.28 (d, ^3J = 6.6 Hz, 12H, CH_3-*i*Pr), 1.77 (m, 4H, THF), 2.84 (sp, ^3J = 6.6 Hz, 4H, CH-*i*Pr), 3.62 (m, 4H, THF), 7.29 (d, ^3J = 7.7 Hz, 4H, Ar(*m*-H)), 7.34 (s, 2H, Im(H)), 7.41 (t, ^3J = 7.7 Hz, 2H, Ar(*p*-H)); ^{13}C NMR (125 MHz, d_8-THF): -17.6 (MgMe), 22.4 (CH_3-*i*Pr), 22.6 (CH_3-*i*Pr), 23.5 (THF), 26.5 (CH-*i*Pr), 64.9 (THF), 121.6 (Im(CH)), 121.6 (Ar(CH)) 127.4 (Ar(CH)), 134.9 (Ar), 146.0 (Ar(C_{ipso})),186.6 (carbene).

Preparation of [Mg(IPr)(Me)$_2$(THF)] (5). In a glovebox, 1 equiv. of methyllithium in hexane solution (80 μL, 0.12 mmol) was slowly added to a cold solution (-35 °C) of 1 equiv. of [Mg(IPr)(Me)(Br)(THF)] (**5**) (0.045 g, 0.12 mmol) solubilized in 1 ml of THF. The formation of a precipitate was observed after 15 min while the solution had turned orange. After filtration over a plug of kieselguhr, the solution was dried out. The residues were washed with pentane to afford **6** as a white powder (0.037 g, 75 %). ^{1}H NMR (500 MHz, d_8-THF): -1.93 (s, 6H, $MgMe_2$), 1.16

(d, ^3J = 6.8 Hz, 12H, CH_3-*i*Pr), 1.22 (d, ^3J = 6.8 Hz, 12H, CH_3-*i*Pr), 1.77 (m, 4H, THF), 2.82 (sp, ^3J = 6.7 Hz, 4H, CH-*i*Pr), 3.62 (m, 4H, THF), 7.25 (s, 2H, Im(H)), 7.27 (d, ^3J = 7.8 Hz, 4H, Ar(*m*-H)), 7.38 (t, ^3J = 7.8 Hz, 2H, Ar(*p*-H)); ^{13}C NMR (125 MHz, d_8-THF): -15.9 ($MgMe_2$), 24.1 (CH_3-*i*Pr), 24.4 (CH_3-*i*Pr), 26.1 (THF), 29.0 (CH-*i*Pr), 68.0 (THF) , 123.3 (Ar(CH)), 123.9 (Im(CH)), 129.5 (Ar(CH)), 138.4 (Ar), 146.6 (Ar(C_{ipso})).

Preparation of [{(Mg(IMes)(Br)}$_2$(μ-Me)$_2$] (6). Procedure 1: In a glovebox, 1.05 equiv. of methylmagnesium bromide in Et_2O solution (0.4 ml, 1.10 mmol) was added dropwise to 1 equiv. of free IMes (0.318 g, 1.04 mmol) dissolved in 5 ml of toluene and 5 ml of diethyl ether (1:1) at -35 °C. After 4 hours at room temperature, a precipitate was formed and the solvents were removed under reduced pressure. Two triturations/filtrations made with 10 ml of solutions containing 1:5 volumes of toluene:pentane, followed by one trituration/filtration made with 5 ml of pentane produced **6** as a white powder (0.376 g, 85 %). ^{1}H NMR (500 MHz, C_6D_5Br): -1.96 (s, 3H, MgMe), 2.00 (s, 12H, Ar(*o*-Me)), 2.22 (s, 6H, Ar(*p*-Me)), 6.44 (s, 2H, Im(CH)), 6.64 (s, 4H, Ar(*m*-H)); ^{13}C{^{1}H} NMR (125 MHz, C_6D_5Br): -14.9 (MgMe), 17.6 (Ar(*o*-Me)), 21.0 (Ar(*p*-Me)), 118.0 (Im(CH)), 134.6 (Ar), 135.0 (Ar), 138.4 (Ar), 182.0 (carbene).

Procedure 2: In a glovebox, 1 equiv. of anhydrous magnesium bromide (0.193 g, 1.05 mmol) was added to 12 mL of diethyl ether containing 1 equiv. of free IMes (0.320 g, 1.05 mmol). The solution was stirred until dissolution of $MgBr_2$ and cooled down to -35°C. Then 1.05 equiv. of methyllithium in Et_2O solution (0.4 ml, 1.10 mmol) was added dropwise. After 1 hour at room temperature, a precipitate attributed to the formation of LiBr was discarded upon filtration through a glass frit (porosity 5) and the solvent was removed under pressure. The residues were twice triturated/filtered with 10 ml of a solution containing 1:5 volumes of toluene:pentane, and once with 5 ml of pentane yielding **7** as a white powder (0.141 g, 32 %).

Preparation of [(Mg(IPr)(Br)(μ-Me)]$_2$ (7). Following the protocol 1 used for **6**, 1 equiv. of methylmagnesium bromide in Et_2O solution (0.3 ml, 0.87 mmol) and 1 equiv. of free IPr (0.320 g, 0.87 mmol) produced **7** as a white powder (0.340 g, 81 %). ^{1}H NMR (500 MHz, C_6D_5Br): -2.07 (s, 3H, MgMe), 0.94 (d, ^3J = 6.6 Hz, 12H, CH_3-*i*Pr), 1.37 (d, ^3J = 6.6 Hz, 12H, CH_3-*i*Pr), 2.80 (sp, ^3J = 6.6 Hz, 4H, CH-*i*Pr), 6.82 (s, 2H, Im(CH)), 7.03 (d, ^3J = 7.6 Hz, 4H, Ar(*m*-H)), 7.22 (t, ^3J = 7.6 Hz, 2H, Ar(*p*-H)); ^{13}C{^{1}H} NMR (125 MHz, C_6D_5Br): -14.2 (MgMe), 23.3

(CH_3-*i*Pr), 25.6 (CH_3-*i*Pr), 28.1 (CH-*i*Pr), 123.7 (Im(CH)), 130.1 (Ar), 134.7 (Ar), 145.5 (Ar), 185.0 (carbene).

Preparation of [{(Mg(IMes)(Ph)}$_2$(μ-Br)$_2$] (8). Following the protocol 1 used for **7**, 1.06 equiv. of phenylmagnesium bromide in Et_2O solution (0.3 ml, 0.95 mmol) and 1 equiv. of free IMes (0.275 g, 0.90 mmol) produced **8** as a white powder (0.424 g, 78 %). ^{1}H NMR (500 MHz, C_6D_5Br): 1.83 (s, 12H, Ar(*o*-Me)), 2.16 (s, 6H, Ar(*p*-Me)), 5.84 (s, 2H, Im(CH)), 6.62 (s, 4H, Ar(*m*-H)), 7.39 (m, 3H, MgPh), 7.59 (m, 2H, MgPh); ^{13}C{^{1}H} NMR (125 MHz, C_6D_5Br): 17.3 (Ar(*o*-Me)), 20.8 (Ar(*p*-Me)), 121.8 (Im(CH)), 124.8 (Ar), 134.5 (Ar), 134.5 (Ar), 138.2 (Ar), 139.8 (Ar), 167.0 (Ar), 181.9 (carbene).

Preparation of [{(Mg(IMes)(Bn)}$_2$(μ-Cl)$_2$] (9). Following the protocol 1 used for **7**, 1.05 equiv. of benzylmagnesium chloride in Et_2O solution (1.1 ml, 1.07 mmol) and 1 equiv. of free IMes (0.310 g, 1.02 mmol) produced **9** as a white powder (0.406 g, 82 %). ^{1}H NMR (500 MHz, C_6D_5Br): 1.43 (s, 2H, Bn(CH_2)), 1.89 (s, 12H, Ar(*o*-Me)), 2.13 (s, 6H, Ar(*p*-Me)), 5.88 (s, 2H, Im(CH)), 6.73 (s, 4H, Ar(*m*-H)), 6.90 (t, 1H, Bn(*p*-CH)), 7.20 (t, 2H, Bn(*m*-CH)), 7.25 (d, 2H, Bn(*o*-CH); ^{13}C{^{1}H} NMR (125 MHz, C_6D_5Br): 17.4 (Ar(*o*-Me)), 21.0 (Ar(*p*-Me)), 63.4 (Bn), 122.2 (Im(CH)), 124.7 (Ar), 126.7 (Ar), 129.1 (Ar), 134.6 (Ar), 134.7 (Ar), 138.0 (Ar), 146.7 (Ar), 182.9 (carbene).

Preparation of [{(Mg(IPr)(Ph)}$_2$(μ-Br)$_2$] (10). Following the protocol 1 used for **7**, 1 equiv. of phenylmagnesium bromide in Et_2O solution (0.3 ml, 0.80 mmol) and 1 equiv. of free IPr (0.312 g, 0.80 mmol) produced **10** as a white powder (0.298 g, 65 %). ^{1}H NMR (500 MHz, C_6D_5Br): 1.09 (d, ^3J = 6.6 Hz, 12H, CH_3-*i*Pr), 1.15 (d, ^3J = 6.6 Hz, 12H, CH_3-*i*Pr), 2.62 (sp, ^3J = 6.6 Hz, 4H, CH-*i*Pr), 7.26 (s, 2H, Im(CH)), 7.52 (d, ^3J = 7.6 Hz, 4H, Ar(*m*-H)), 7.60 (m, 3H, MgPh), 7.71 (t, ^3J = 7.6 Hz, 2H, Ar(*p*-H)), 8.02 (m, 2H, MgPh).

Preparation of [{(Mg(IMes)(Br)}$_2$(μ-Cl)$_2$] (11). In a glovebox, 1.2 equiv. of ethylmagnesium bromide in Et_2O solution (0.70 ml, 0.74 mmol) was added dropwise to a vigorously stirred slurry of 1.0 equiv. of IMesHCl (0.211 g, 0.62 mmol) in 10 ml of THF. Progressive dissolution of the imidazolium salt was observed simultaneously with formation of ethane bubbling. The resulting orange solution was stirred for 2 h. Upon removal of the solvent under reduced pressure, a white powder was obtained and washed with 10 ml of pentane, to afford the complex **11** (0.274 g, 85

%). ^{1}H NMR (500 MHz, d_8-THF): 1.77 (m, 4H, THF), 2.16 (s, 12H, Ar(*o*-Me)), 2.33 (s, 6H, Ar(*p*-Me)), 3.62 (m, 4H, THF), 7.02 (s, 4H, Ar(*m*-H)), 7.31 (s, 2H, Im(H)); ^{13}C{^{1}H} NMR (125 MHz, d_8-THF): 18.0 (Ar(*o*-Me)), 20.9 (Ar(*p*-Me)), 26.2 (THF), 68.0 (THF), 123.4 (Im(CH)), 129.5 (Ar(CH)), 136.3 (Ar), 136.3 (Ar), 139.4 (Ar(C_{ipso})), 187.0 (carbene).

Preparation of $[Mg(IMes)(Me)(THF)_2]^+[(B(C_6H_5)_4]^-$ (12). In a glovebox, 1 equiv. of $NaBPh_4$ (0.168 g, 0.56 mmol) and 5 equiv. of THF (0.23 ml, 2.8 mmol) were added to10 ml of fluorobenzene containing 1 equiv. of [Mg(IMes)(Me)(Br)(THF)] (**3**) (0.280 g, 0.56 mmol). After 12 hours at room temperature, a precipitate was formed and the solvents were removed under reduced pressure. Three triturations/filtrations made with 10 ml of pentane produced **12** as a white powder (0.414 g, 83%). ^{1}H NMR (400 MHz, C_6D_5Br): -1.62 (s, 3H, MgMe), 1.18 (m, 8H, THF), 1.84 (s, 12H, Ar(*o*-Me)), 2.15 (s, 6H, Ar(*p*-Me)), 2.88 (m, 8H, THF), 6.74 (t, ^{3}J = 7.2 Hz, 4H, BPh(*p*-H)), 6.94 (t, ^{3}J = 7.4 Hz, 8H, BPh(*m*-H)), 7.05 (s, 4H, Ar(*m*-H)), 7.15 (s, 2H, Im(H)), 7.33 (m, 8H, BPh(*o*-H)); ^{13}C{^{1}H} NMR (125 MHz, C_6D_5Br) -15.7 (MgMe), 17.1 (Ar(*o*-Me)), 20.8 (THF), 24.1 (Ar(*p*-Me)), 69.4 (THF), 121.5 (BPh(CH)), 124.2 (Im(CH)), 125.4 (m, BPh(CH)), 129.7 (Ar(CH)), 135.9 (Ar), 136.2 (Ar), 136.8 (BPh(CH)), 139.9 (Ar(C_{ipso})), 164.8 (m, BPh(C_{ipso})), 179.1 (carbene); ^{11}B NMR (128 MHz, C_6D_5Br) -5.9 (BPh_4).

Preparation of $[Mg(IPr)(Me)(THF)_2]^+[(B(C_6H_5)_4^-]$ (13). Following a protocol used for **12**, 1 equiv. of $NaBPh_4$ (0.180 g, 0.54 mmol), 5 equiv. of THF (0.21 ml, 2.7 mmol) and 1 equiv. of [Mg(IPr)(Me)(Br)(THF)] (**5**) (0.300 g, 0.54 mmol) produced **13**, as a white powder (0.389 g, 81 %). ^{1}H NMR (500 MHz, C_6D_5Br): -1.70 (m, 2H, MgMe), 1.00 (d, ^{3}J = 6.6 Hz, 12H, CH_3-*i*Pr), 1.12 (d, ^{3}J = 6.6 Hz, 12H, CH_3-*i*Pr), 1.19 (m, 8H, THF), 2.48 (sp, ^{3}J = 6.6 Hz, 4H, CH-*i*Pr), 2.85 (m, 8H, THF), 6.75 (s, 2H, Im(H)), 6.96 (t, ^{3}J = 7.1 Hz, 4H, BPh(*p*-H)), 7.13 (t, ^{3}J = 7.4 Hz, 8H, BPh(*m*-H)), 7.31 (d, ^{3}J = 7.7 Hz, 4H, Ar(*m*-H)), 7.42 (t, ^{3}J = 7.7 Hz, 2H, Ar(*p*-H)), 7.78 (m, 8H, BPh(*o*-H)),; ^{13}C NMR (125 MHz, C_6D_5Br): -15.9 (MgMe), 22.3 (THF), 23.8 (CH_3-*i*Pr), 29.0 (CH-*i*Pr), 69.2 (THF), 121.5 (BPh(CH)), 124.2 (Im(CH)), 124.4 (Ar(CH)), 125.4 (m, BPh(CH)), 130.1 (Ar(CH)), 136.8 (BPh(CH)), 137.4 (Ar), 146.5 (Ar(C_{ipso})) 164.4 (m, BPh(C_{ipso})), 181.6 (carbene); ^{11}B NMR (128 MHz, C_6D_5Br) -5.9 (BPh_4).

Preparation of [{[Mg(IMes)(Me)][Mg(IMes)]}(μ-Me)$_2$]$_2$(μ-Br)$_2$]$^{2+}$[(B(C$_6$F$_5$)$_4$]$^-_2$ (14). In a glovebox, 1 equiv. of Li[B(C$_6$F$_5$)$_4$] (0.123 g, 0.18 mmol) was added to 10 ml of bromobenzene containing 1 equiv. of [{(Mg(IMes)(Br)}$_2$(μ-Me)$_2$] (**7**) (0.087 g, 0.09 mmol). A white precipitate was immediately observed upon addition of the sodium salt. After filtration over Kieselguhr, the resulting solution was cooled at -35 °C providing **14** as colourless crystals. (0.063 g, 22 %). ^{1}H NMR (400 MHz, C$_6$D$_5$Br): -2.63 (s, 3H, MgMe), 1.82 (s, 24H, Ar(*o*-Me)), 2.20 (s, 12H, Ar(*p*-Me)), 6.62 (s, 4H, Im(H)), 6.71 (s, 4H, Mes), 6.79 (s, 8H, Mes); ^{13}C{^{1}H} NMR (125 MHz, C$_6$D$_5$Br) -16.9 (MgMe), 16.7 (Ar(*o*-Me)), 20.6 (Ar(*p*-Me)), 127.7 (Ar), 137.3 (Ar), 139.0 (Ar), 141.8 (Ar), 142.7 (Ar), 148.8 (Ar), 175.3 (carbene).

Associated content

Supporting information

NMR spectra of complexes **1-14**, summary of crystal data for **5', 6, 7, 8, 9, 10, 11, 12', 13**, computational details on models **V'**, **VI**, **VII**, **XII'** and **XIII**. The Crystallographic information files (CIF) have been deposited with the CCDC, 12 Union Road, Cambridge, CB2 1EZ, U.K., and can be obtained on request free of charge, by quoting the publication citation and deposition numbers 1906336 & 1906341–1906349. This material is also available free of charge via the Internet at http://pubs.acs.org.

Author information

Corresponding Authors

*E-mail: dagorne@unistra.fr; defremont@unistra.fr

ORCID

Samuel Dagorne: 0000-0001-7393-286X

Pierre de Frémont: 0000-0001-8470-3659

Lydia Karmazin : 0000-0003-0416-6190

Laurent Ruhlmann: 0000-0003-1154-2422

Acknowledgment

The Centre National de la Recherche Scientifique (CNRS), The University of Strasbourg and the Ministère de l'Enseignement Supérieur et de la Recherche (Ph.D. fellowship to J.C.B) are gratefully acknowledged for support. The NMR service of the Université de Strasbourg is warmly acknowledged for the various studies.

Notes

The authors declare no competing financial interest.

References

1. Grignard, V. Sur quelques nouvelles combinaisons organométalliques du magnésium et leur application à des synthèses d'alcools et d'hydrocarbures. *C. R. Hebd. Séances Acad. Sci.* **1900**, 1322–1325.

2. *The Chemistry of Organomagnesium Compounds*, Eds. : Rappoport, Z.; Marek, I.; Wiley-VCH, Weinheim, **2008**.

3. Seyferth, D. The Grignard Reagents. *Organometallics* **2009**, *28*, 1598–1605.

4. Selected reviews/books on NHCs: (a) N-Heterocyclic Carbenes: Effective Tools in Organometallic Synthesis, Ed.: Nolan, S. P.; Wiley-VCH,Weinheim, **2014**. (b) Bourissou, D.; Guerret, O.; Gabbaï, F.; Bertrand, G. Stable Carbenes *Chem. Rev.* **2000**, *100*, 39–92. c) W. A. Herrmann *N*- Heterocyclic Carbenes: A New Concept in Organometallic Catalysis. *Angew. Chem. Int. Ed.* **2002**, *41*, 1290–1309. d) César, V.; Bellemin-Laponnaz, S.; Gade, L. H. Chiral N-heterocyclic carbenes as stereodirecting ligands in asymmetric catalysis. *Chem. Soc. Rev.* **2004**,

33, 619; e) de Frémont, P.; Marion, N.; Nolan, S. P. Carbenes: Synthesis, Properties, and Organometallic Chemistry. *Coord. Chem. Rev.* **2009**, *253*, 862–892. (f) Fliedel, C.; Schnee, G.; Avilés, T.; Dagorne, S. Group 13 metal (Al, Ga, In, Tl) complexes supported by heteroatom-bonded carbene ligands. *Coord. Chem. Rev.* **2014**, *275*, 63–86.

5. Bellemin-Laponnaz, S.; Dagorne, S. Group 1 and 2 and Early Transition Metal Complexes Bearing N-Heterocyclic Carbene Ligands: Coordination Chemistry, Reactivity, and Applications *Chem. Rev.* **2014**, *114*, 8747–8774.

6. Nesterov, V.; Reiter, D.; Bag, P.; Frisch, P.; Holzner, R.; Porzelt, A.; Inoue, S. NHCs in Main Group Chemistry. *Chem. Rev.* **2018**, *118*, 9678–9842.

7. Arduengo, A. J.; Dias, H. V. R.; Davidson, F.; Harlow, R. L. Carbene Adducts of Magnesium and Zinc. *J. Organomet. Chem.* **1993**, *462*, 13–18.

8. Selected representative examples of NHC-Mg species: (a) Arduengo, A. J.; Davidson, F.; Krafczyk, R.; Marshall, W. J.; Tamm, M. Adducts of Carbenes with Group II and XII Metallocenes †. *Organometallics* **1998**, *17*, 3375–3382. (b) Mungur, S. A.; Liddle, S. T.; Wilson, C.; Sarsfield, M. J.; Arnold, P. L. Bent metal carbene geometries in amido N-heterocyclic carbene complexes. *Chem. Commun.* **2004**, *23*, 2738−2739. (c) Zhang, D.; Kawaguchi, H. Deprotonation Attempts on Imidazolium Salt Tethered by Substituted Phenol and Construction of Its Magnesium Complex by Transmetalation. *Organometallics* **2006**, *25*, 5506−5509. (d) Kennedy, A. R.; Klett, J.; Mulvey, R. E.; Robertson, S. D. N-Heterocyclic-Carbene-Induced Monomerization of Sterically Encumbered Dialkylmagnesium and Dialkylmanganese Polymers. *Eur. J. Inorg. Chem.* **2011**, *2011*, 4675–4679. (e) Arrowsmith, M.; Hill, M. S.; MacDougall, D. J.; Mahon, M. F. A Hydride-Rich Magnesium Cluster. *Angew. Chem. Int. Ed.* **2009**, *48*, 4013–4016. (f) Ghadwal, R. S.; Rottschäfer, D.; Schürmann, C. J. Expedient Access to Normal- and Abnormal- N-Heterocyclic Carbene (NHC) Magnesium Compounds from Imidazolium Salts: Expedient Access to Normal- and Abnormal- N-Heterocyclic Carbene (NHC) Magnesium Compounds from Imidazolium Salts. *Z. Für Anorg. Allg. Chem.* **2016**, *642*, 1236–1240. (g)

Baishya, A.; Peddarao, T.; Nembenna, S. Organomagnesium Amide Catalyzed Cross-Dehydrocoupling of Organosilanes with Amines. *Dalton Trans.* **2017**, *46*, 5880–5887. (h) Wong, Y. O.; Freeman, L. A.; Agakidou, A. D.; Dickie, D. A.; Webster, C. E.; Gilliard Jr., R. J. Two Carbenes versus One in Magnesium Chemistry: Synthesis of Terminal Dihalide, Dialkyl, and Grignard Reagents. *Organometallics* **2019**, *38*, 688–696. (i) Kennedy, A. R.; Mulvey, R. E.; Robertson, S. D. N-Heterocyclic Carbene Stabilized Adducts of Alkyl Magnesium Amide, Bisalkyl Magnesium and Grignard Reagents: Trapping Oligomeric Organo s-Block Fragments with NHCs. *Dalton Trans.* **2010**, *39*, 9091–9099.

9. For use of Mg-NHC complexes in catalysis, see: (a) Arnold, P. L.; Casely, I. J.; Turner, Z. R.; Bellabarba, R.; Tooze, R. B. Magnesium and Zinc Complexes of Functionalised, Saturated N-Heterocyclic Carbene Ligands: Carbene Lability and Functionalisation, and Lactide Polymerisation Catalysis. *Dalton Trans.* **2009**, 7236–7247. (b) Antu, B.; Manohar Pawar, G.; Wurst, K.; Decker, U.; Schmidt, A. M.; Buchmeiser, M. R. CO_2, Magnesium, Aluminum, and Zinc Adducts of N-Heterocyclic Carbenes as (Latent) Catalysts for Polyurethane Synthesis. *Eur. J. Inorg. Chem.* **2009**, 1970−1976. (c) Okamoto, S.; Ishikawa, H.; Shibata, Y.; Suhara, Y. Grignard Allylic Substitution Catalyzed by Imidazol-2-Ylidene- and Imidazol-4-Ylidene-Magnesium Complexes. *Tetrahedron Lett.* **2010**, *51*, 5704–5707. (b) Baishya, A.; Barman, M. K.; Peddarao, T.; Nembenna, S. Catalytic C–N Bond Formation in Guanylation Reaction by N-Heterocyclic Carbene Supported Magnesium(II) and Zinc(II) Amide Complexes. *J. Organomet. Chem.* **2014**, *769*, 112–118.

10. Recent representative examples of discrete Mg species in catalysis: (a) Rauch, M.; Ruccolo, S.; Parkin, G. Synthesis, Structure, andReactivity of a Terminal Magnesium Hydride Compound with a Carbatrane Motif, [TismPriBenz]MgH: A Multifunctional Catalyst for Hydrosilylation and Hydroboration. *J. Am. Chem. Soc.* **2017**, *139*, 13264−13267. (b) Anker, M. D.; Arrowsmith, M.; Bellham, P.; Hill, M. S.; Kociok-Köhn, G.; Liptrot, D. J.; Mahon, M. F.; Weetman, C. Selective reduction of CO_2 to a methanol equivalent by $B(C_6F_5)_3$-activated alkaline earth catalysis. *Chem. Sci.* **2015**, *5*, 2826–2830. (c) Lampland, N. L.; Pindwal, A.; Neal, S. R.; Schlauderaff, S.; Ellern, A.; Sadow, A. D. Magnesium-catalyzed hydrosilylation of α,β-unsaturated esters. *Chem. Sci.* **2015**, *6*, 6901–6907. (d) Bellham, P.; Hill, M. S.; Kociok-Köhn, G.; Liptrot, D. J. Bespoke

synthesis of unsymmetrical diaminoboranes by alkaline earth catalysis. *Chem. Commun.* **2013**, *49*, 1960–1962. (e) Baishya, A; Kumar, L.; Barman, M. Kr.; Biswal, H. S.; Nembenna, S. N-Heterocyclic Carbene-Carbodiimide ("NHC-CDI") Adduct or Zwitterionic-Type Neutral Amidinate-Supported Magnesium(II) and Zinc(II) Complexes *Inorg. Chem.* **2017**, *56*, 9535–9546.

11. Review: Hill, M. S.; Liptrot, D. J.; Weetman, C. Alkaline earths as main group reagents in molecular catalysis. *Chem. Soc. Rev.* **2016**, *45*, 972–988.

12. Selected cationic Mg(II) complexes: (a) Juergen, P. ; Stennett, T. E.; Volland, M.; Guldi, D. M.; Harder, S. Complexation and Versatile Reactivity of a Highly Lewis Acidic Cationic Mg Complex with Alkynes and Phosphines. *Chem. Eur. J.* **2019**, 25, 2025–2034. (b) Friedrich, A.; Pahl, J.; Elsen, H.; Harder, S. Bulky cationic *β*-diketiminate magnesium complexes. *Dalton Trans.* **2019**, *48*, 5560–5568. (c) Pahl, J.; Friedrich, A.; Elsen, H.; Harder, S. Cationic Magnesium π-Arene Complexes *Organometallics* **2018**, *37*, 2901–2909. (d) Pahl, J.; Brand, S.; Elsen, H.; Harder, S. Highly Lewis acidic cationic alkaline earth metal complexes *Chem. Commun.* **2018**, *54*, 8685–8688. (e) Rauch, M.; Parkin, G. Zinc and Magnesium Catalysts for the Hydrosilylation of Carbon Dioxide *J. Am. Chem. Soc.* **2017**, *139*, 18162–18165. (f) Wheaton, C. A.; Hayes, P. G. Designing cationic zinc and magnesium catalysts for coordination–insertion polymerization of lactide *Comments Inorg. Chem.* **2011**, *32*, 127–162. (g) Sarazin, Y.; Schormann, M.; Bochmann, M. Novel Zinc and Magnesium Alkyl and Amido Cations for Ring-Opening Polymerization Reactions. *Organometallics* **2004**, *23*, 3296–3302.

13. (a) Specklin, D.; Hild, F.; Fliedel, C.; Gourlaouen, C.; Veiros, L. F.; Dagorne, S. Accessing Two-coordinate Zn(II) Organocations by NHC coordination: Synthesis, Structure, and Use as π-Lewis acids in alkene, alkyne and CO_2 hydrosilylation. *Chem. Eur. J.* **2017**, *23*, 15908–15912. (b) Specklin, D.; Fliedel, C.; Gourlaouen, C.; Bruyere, J.-C.; Avilés, T.; Boudon, C.; Ruhlmann, L.; Dagorne, S. N-Heterocyclic Carbene Based Tri-organyl-Zn-Alkyl Cations: Synthesis, Structures, and Use in CO_2 Functionalization *Chem. Eur. J.* **2017**, *23*, 5509–5519.

14. Mantina, M.; Chamberlin, A.C.; Valero, R.; Cramer, C. J.; Truhlar, D. G. Consistent van der Waals Radii for the Whole Main Group. *J. Phys. Chem. A* **2009**, *113*, 5806–5812.

15. Stasch, A.; Jones, C. Stable dimeric magnesium(I) compounds: from chemical landmarks to versatile reagents. *Dalton Trans.* **2011**, *40*, 5659.

16. Tapu, D.; Dixon, D. A.; Roe, C. ^{13}C NMR Spectroscopy of "Arduengo-type" Carbenes and Their Derivatives. *Chem. Rev.* **2009**, *109*, 3385–3407.

17. (a) Green, S. P.; Jones, C.; Stasch, A. Stable Adducts of a Dimeric Magnesium(I) Compound. *Angew. Chem. Int. Ed.* **2008**, *47*, 9079–9083; (b) Bonyhady, S. J.; Jones, C.; Nembenna, S.; Stasch A.; Edwards, A. J.; McIntyre, G. J. β-Diketiminate-Stabilized Magnesium(I) Dimers and Magnesium (II) Hydride Complexes: Synthesis, Characterization, Adduct Formation, and Reactivity Studies. *Chem. Eur. J.* **2010**, *16*, 938–955.

18. Michalczyk, M. J. Synthesis of magnesium hydride by the reaction of phenylsilane and dibutylmagnesium *Organometallics* **1992**, *11*, 2307–2309.

19. Perdew, J. P.; Burke, K.; Ernzerhof, M. Generalized Gradient Approximation Made Simple. *Phys. Rev. Lett.* **1996**, *77*, 3865–68.

20. Ditchfield, R.; Hehre, W. J.; Pople, J. A. Self- Consistent Molecular- Orbital Methods. IX. An Extended Gaussian- Type Basis for Molecular- Orbital Studies of Organic Molecules. *J. Chem. Phys.* **1971**, *54*, 724–728.

21. For shorter calculation time, for larger models **V**, **VII** and **XII'**, single points were performed on simplified structures with the replacement of N-Dipp/N-Mes substituents by N-Me.

22. (a) Arduengo III, A. J.; Dias, H. V. R.; Harlow, R. L.; Kline, M. Electronic stabilization of nucleophilic carbenes. *J. Am. Chem. Soc.* **1992**, *114*, 5530. (b) Jafarpour, L.; Stevens, E. D.; Nolan, S. P. A sterically demanding nucleophilic carbene: 1,3-bis(2,6-

diisopropylphenyl)imidazol-2-ylidene). Thermochemistry and catalytic application in olefin metathesis. *J. Organomet. Chem*. **2000**, *606*, 49.

23. Sheldrick, G. M. A Short History of SHELX. *Acta Crystallogr. A* **2008**, *64*, 112–122.

24. Sheldrick, G. M. SHELXT - Integrated space-group and crystal-structure determination. *Acta Cryst. A* **2015**, *71*, 3–8.